SiC Microsphere Derived from Phenolic Resin—Ethyl Silicate Heterogeneous Precursors with Carbothermic Reduction

Masaki Narisawa,[1] Hiroshi Ukon,[1] Hiroshi Mabuchi,[1] Kiyohito Okamura,[1] Yasuo Kurachi[2]

[1]Graduate School of Engineering, Osaka Prefecture University 1–1, Gakuen-Cho, Sakai 599-8531, Japan
[2]Konica Minolta Technology Center, Inc., No. 1 Sakura-machi, Hino-shi, Tokyo 191-8511, Japan

ABSTRACT: Heterogeneous precursors for SiC particles were synthesized from viscous phenolic resin and tetraethyl orthosilicate with hastening ethanol removal process in a concentrated state. In the pyrolysis products, spherical carbon domains with diameter of several micrometers were embedded in the SiO_2-C matrix. After the carbothermic reduction process at 2073 K, SiC-C spheres were obtained with an SiC yield of ~80%, while the carbon domains acted as templates of the SiC-C spheres with complete disappearance of the SiO_2-C matrix area. After the carbon burned out, some of the spheres possessed a hollow structure. © 2004 Wiley Periodicals, Inc. J Appl Polym Sci 94: 1612–1618, 2004

Key words: silicas; resins; pyrolysis; phase separation; templates

INTRODUCTION

Recently, the precursor method has become one of the useful processes for synthesizing silicon carbide powder of good quality. This is mainly based on the sol-gel process, which can combine a silicate and a carbon source polymer in nanoscales.[1–3] For the carbon source polymer, phenolic resin has been widely investigated.[4,5] By adjusting a kind of phenolic resin, an alkoxide, and mixing conditions, a homogeneous transparent precursor can be obtained. Kurachi and co-workers demonstrated the important combination of water-soluble, low-viscosity phenolic resin with toluene sulfonic acid catalyst, which bring the strong interaction between the partially hydrolyzed silicate and the phenolic resin.[6,7] The precursor thus tailored yields SiC nanocrystallites with nucleation and crystal growth mechanisms in an analogous Si-C-O amorphous.[6–8] The morphology of the resulting particle depends on heat treatment conditions at 1873–2073 K in an inert atmosphere as well as the starting precursor compositions.[9] High SiC yield with reducing SiO loss is also remarkable.

The combinations of the thermosetting resin and the alkoxide, including the phenolic resin–tetraethyl orthosilicate (TEOS) system, are known to often yield apparent phase separation because of the low miscibility of the resins and the hydrolyzed silicates.[10] In ordinary cases, the silica domains in nano- or microscales were embedded in the resin matrix in the observed microstructure.

During investigation on various microstructures of phenolic resin–TEOS systems, we found a considerably rare microstructure, in which spherical resin domains were dispersed in a silicate-rich matrix. This unique microstructure can be formed by using a viscous phenolic resin for the carbon source with hastening ethanol removal process during the hydrolysis reaction. Such a microstructure is probably determined by the phase separation process in the concentrated state. A phenomenon of phase separation often yields unique patterns, like a dispersed sphere, partially percolated agglomerate, lamella, and cylinder in the cases of polymer blends[11,12] and sol-gel processes.[13,14] Even in the case of silicon carbide base ceramic materials, some phase separation patterns of Si-C backbone polymer blend systems (allylhydridopolycarbosilane, AHPCS) was characterized and the SiC ceramic synthesis with controlled microstructures using such polymer blend natures was mentioned.[15]

We expected the mass production of SiC microbuildings with controlled morphology using the phenolic resin–silicate phase separation pattern to be an "active" template. This process is economical compared with the use of precious organosilicon polymers, which need alumina or silica templates for constructing microbuildings (nanofiber, network, etc.).[16–18] The microbuildings (typically spheres) obtained by our method have promising application in

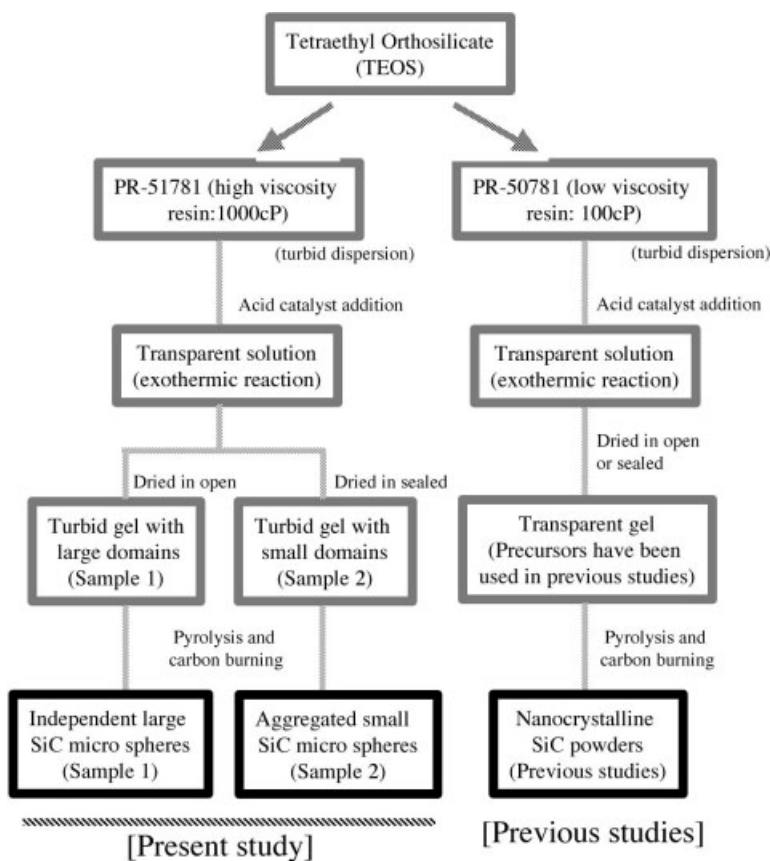*Correspondence to:* M. Narisawa (nar@mtl.osakafu-u.ac.jp).

Figure 1 Flow chart of microsphere synthesis.

the field of heat-insulating ceramic composites with light-weight and semiconductive fillers for conventional ceramic and plastic materials. Applications for heat-resistant diesel particulate filters using its porosity is also promising.

EXPERIMENTAL

In the present study, Sumiliteresin PR-51781 (Sumitomo Bakelite Co. Ltd.) [resin 76%, phenol-alcohol 12.5%, aldehyde 2.5%, water 9.0% in mass, viscosity: 1000 cP] was used to give the heterogeneous precursors. About 30 g of the phenolic resin was dispersed in 70 g of TEOS, and 13.5 mL of toluene sulfonic acid 30% solution was successively added in the solution. With an exothermic reaction with increasing the temperature up to 70°C, a transparent mixture was obtained. After continuous stirring for 30 min, the solution was cast in cylindrical polypropylene cells (28 mm in diameter and 70 mm in height) with a depth of 3 mm.

Sample 1 gels were prepared by drying the mixtures merely in the open state. Sample 2 gels were prepared by storing the mixture for 3 days with polypropylene caps to complete gelation. After the caps were removed, they were dried in the open state. The cross-section of these dried gel sheets was polished and

analyzed by a focused laser Raman spectrum analyzer (Senturion, Chromex). Thus, the obtained gel sheets were pyrolyzed at 1273 K in an N_2 gas flow for 30 min. The cross-section of the pyrolyzed gel sheets was observed and analyzed by electron microprobe analyzer (JXA-870, Jeol).

The pyrolyzed gel sheets were successively heat-treated at 2073 K for 30 min to obtain SiC powders by carbothermic reduction, using a graphite furnace in an Ar gas flow. XRD pattern measurements, SEM observation (S-4500, Hitachi), and TG analysis (TG-8110, Rigaku) in air were performed on the synthesized powders.

The SiC synthesis procedure is shown in Figure 1 in comparison with the previous procedure using PR-50781 resin for carbon source polymer.[8,9] The IR spectrum of PR-51781 resin (for heterogeneous precursor) is shown in Figure 2 with that of the PR-50781 resin (for homogeneous precursors). The spectrum of PR-51781 is almost same as that of PR-50781. The absorption bands at 1515 and 1485 cm^{-1} are, however, strong, while the band at 1020 cm^{-1} is weak. These differences indicate that PR-51,781 contains an increased amount of methylene bridges (-CH$_2$-: 1515 and 1485 cm^{-1}) and a decreased amount of methylol groups (-CH$_2$OH: 1020 cm^{-1}) compared with PR-

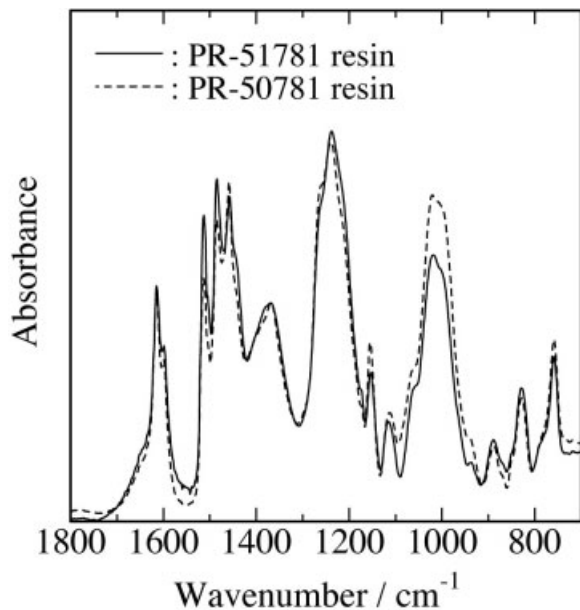**Figure 2** IR spectra of the liquid phenolic resin.

Figure 4 Laser beam analysis of Raman spectra on a domain and matrix area in the dried gel of sample 1 (para: *p*-substituted ring, meta: *m*-substituted ring, these spectra were shown after the fluorescence background was subtracted).

50781.[19–21] PR-51781, with increased viscosity, is intrinsically a high-molecular-weight prepolymer compared with PR-50781.

RESULTS AND DISCUSSION

Although the starting resin–TEOS mixture keeps its transparent appearance, the dried gel sheets show a turbid and red-colored appearance.

Figure 3 shows the photo image of a polished cross-section of a sample 1 gel after drying. Spherical do-
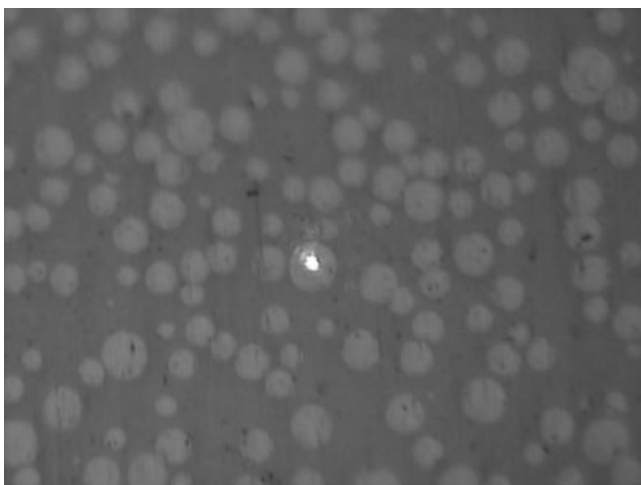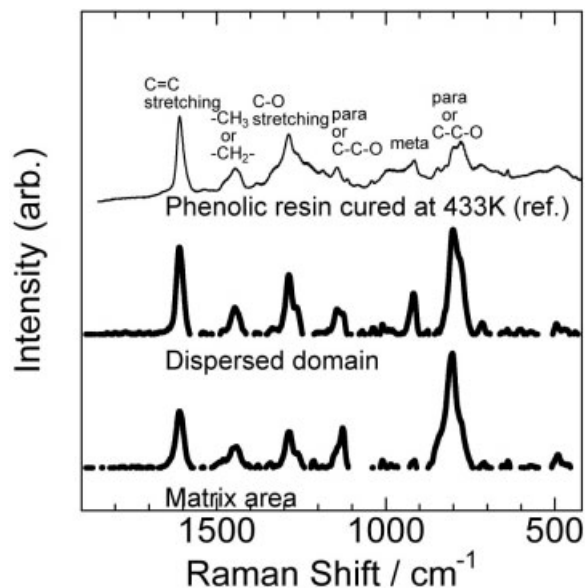

20 μm

Figure 3 A photo image of a polished cross-section of the dried gel of sample 1 (a bright spot at the center shows the laser beam on a large domain).

mains dispersed in the matrix are observed. The results of Raman spectra analysis by focused laser beam on the domains and the surrounding matrix are shown in Figure 4. The spectrum of merely cured resin is also shown in Figure 4 as a reference. In the cured resin, the bands of C = C stretching (1600 cm^{-1}), -CH$_2$- or -CH$_3$ bending (1450 cm^{-1}), C-O stretching (1300 cm^{-1}), ρ-substituted aromatic ring (1120 and 800–750 cm^{-1}), and *m*-substituted aromatic ring are observed.[19–21] These bands also exist in the spectra of the domains and matrix areas. Phenolic resin is suggested to be included in both areas. In the matrix area, however, the bands at 1120 and 800–750 cm^{-1} show considerably high intensity compared with other bands. The C-C-O bond possibly assigned to ethoxyl groups shows Raman bands at almost the same position (1120 and 800–750 cm^{-1}) as the *p*-substituted aromatic ring. Such a small difference in the spectrum would suggest an incomplete hydrolysis reaction of ethyl silicate in the matrix area.

The residual masses of these gel sheets at 1273 K were ~60% for samples 1 and 2. By the pyrolysis at 1273 K, the ethyl silicate–resin precursors are converted to SiO$_2$-C hybrid materials. Carbon burning tests by TG-DTA on these SiO$_2$ = C materials revealed 51.8% and 47.5% carbon contents for sample 1 and 2, respectively. Figure 5(a–c) shows SEM images of samples 1 and 2 after the sample cross-sections were polished. In sample 1, dark spherical domains with a diameter of 5.8 μm (average diameter of large 10 in the area of 120 × 90 μm) was observed [Fig. 5(a)]. This
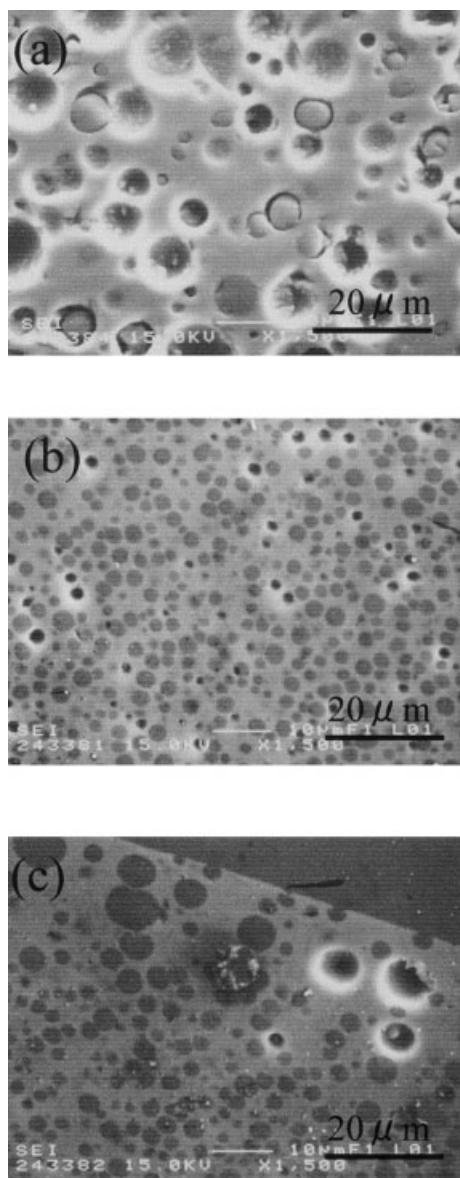
Figure 5 SEM images of polished cross-sections of 1273 K pyrolysis products: (a) product of sample 1; (b) product of sample 2; (c) product of sample 2 (surface area).

average diameter indicates the diameter of circles, which are crosscuts of spheres dispersed in the matrix. Some dimples are also observed on the same surface, which should be caused by dark domain droppings during the polishing procedure. Figure 6 shows the result of line analysis of Si, O, and C using the electron microprobe analyzer across the diameter of a dark domain. A comparatively large domain maintaining good contact with the surrounding matrix was selected for this analysis. This elemental analysis reveals that the dark domain mainly consists of carbon, while the surrounding matrix consists not only of SiO_2 but also of C. For a chemical composition of the matrix, a C/SiO_2 molar ratio of ~2 is suggested.

In sample 2 [Fig. 5(b)], smaller spherical dark domains with a diameter of 3.1 μm (average of large 10 in 120 $\times$ 90 μm) were observed. The number of dimples in the cross-section is relatively small. The dispersed domains probably keep good contact with the matrix during polishing compared with those in sample 1. Spheres with comparatively large size are, however, formed at the vicinity of the surface area [Fig. 5(c)].

The Raman analysis on the dried gels and the elemental line analysis across the carbon-rich domain in the pyrolysis product at 1273 K suggest an occasion of asymmetric phase separation between the partially hydrolyzed silcates and the resin. The resin is incorporated into the silicate networks, perhaps in nanoscales, and is also trapped in the large pores. Such an image is reciprocal to the phenolic resin–silica hybrid structures reported by Haraguchi et al.[10] It is, however, analogous to a kind of macroporous silica gel completely filled with organic compounds, although every pore in our system exists as a closed pore.[22–24] Such macroporous structure was probably determined during the mixture drying process just before gelation, as well as the viscous resin nature, and was maintained during pyrolysis up to 1273 K.

Heat treatments of the pyrolysis products at 2073 K in an Ar atmosphere caused 58.7% mass loss for sample 1 and 54.2% mass loss for sample 2. The sheet form was collapsed during the heat treatment to yield black powders. XRD patterns of the obtained powders reveal the patterns of β-SiC and amorphous carbon. The shoulder at 33.6° in the XRD patterns also suggests the
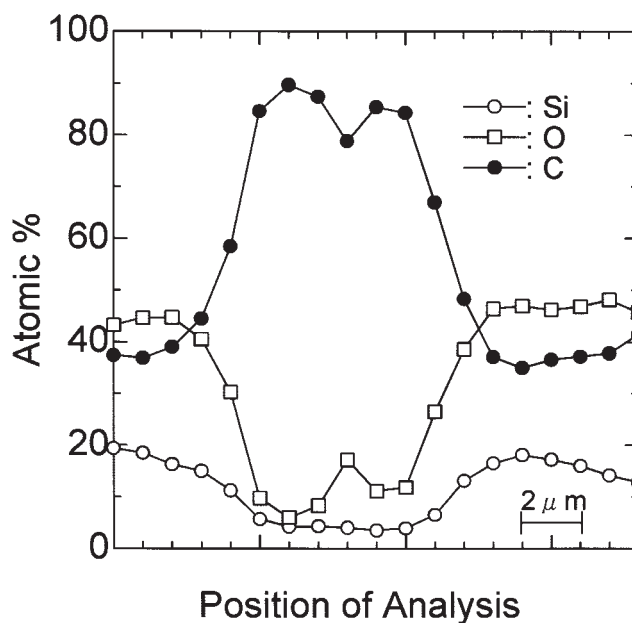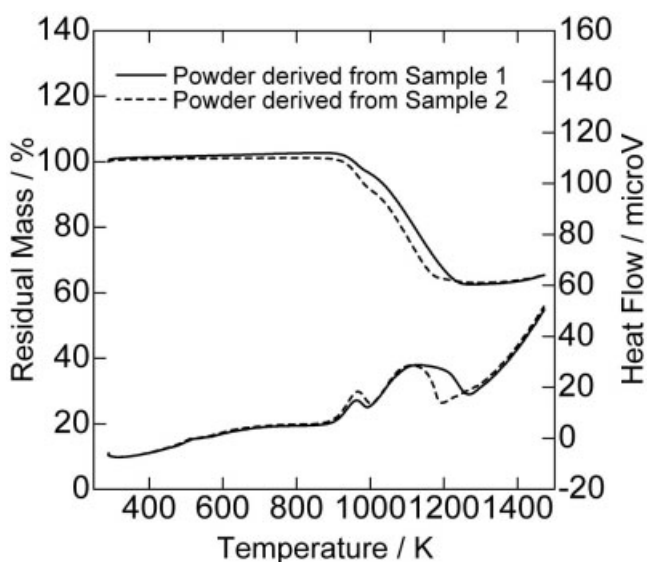

Figure 6 Elemental line analysis by electron microprobe across a C-rich domain (pyrolysis product of sample 1).
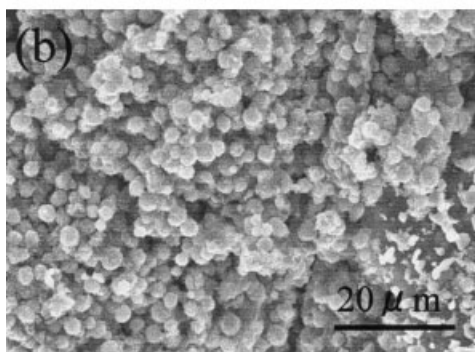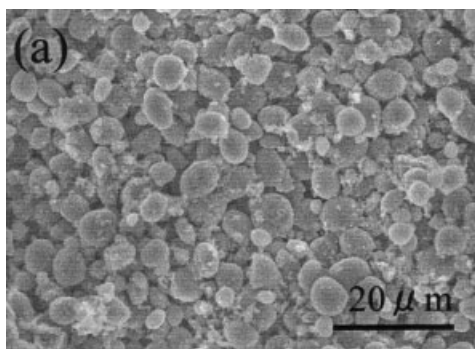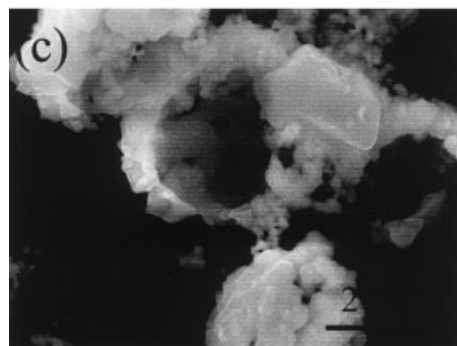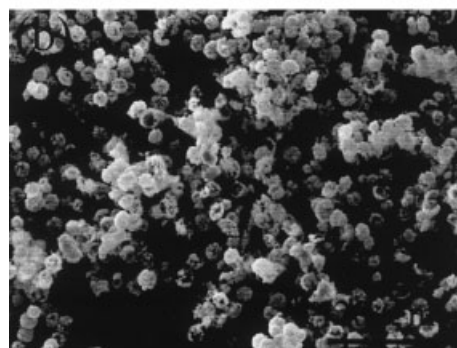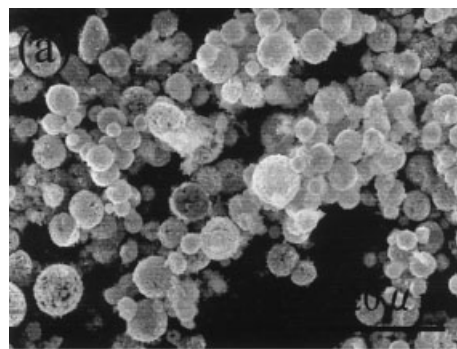
Figure 7 SEM micrographs of the obtained powders: (a) SiC-C powder from sample 1; (b)SiC-C powder from sample 2.

existence of a small amount of stacking faults.[25,26] Figure 7(a,b) shows the SEM images of the obtained powders. Spheres derived from sample 1 are larger than those derived from sample 2. On the other hand, the matrix surrounding the carbon-rich domains completely disappears during SiC formation.

Figure 9 SEM micrographs of the powders after oxidation: (a) partially oxidized SiC powder from sample 1; (b) partially oxidized SiC powder from sample 2; (c) partially oxidized hollow SiC sphere in sample 2 powder (high magnification).


Figure 8 TG-DTA analysis on the obtained SiC-C powders in air (heating rate 10 K/min).

Figure 8 shows TG-DTA curves of the synthesized powders in air. Mass losses with exthothermic reaction at 900–1280 K and continuous mass gains beyond 1280 K are observed. It is natural to assign the sudden mass losses at 900–1280 K to carbon burning and mass gains beyond 1280 K to SiC oxidation. In practical approximation, we assume the mass loss percentage up to 1280 K equal to the carbon contents in the SiC-C powders, which are 37.5 mass % for sample 1 and 37.1 mass % for sample 2.

Figure 9 shows the SEM images of the powders after oxidation at 1473 K (colored gray). Even after

the carbon burning and the partial oxidation, spheres maintain their shapes. In the case of sample 1, each sphere is completely independent [Fig. 9(a)]. Detailed SEM investigation revealed that the individual sphere consists of numerous SiC crystallites. On the other hand, the spheres in sample 2 are not completely independent. In some parts, aggregates of the SiC spheres are observable [Fig. 9(b)]. In an SEM image with high magnification, several hollow spheres with an SiC wall are observed [Fig. 9(c)].

We estimated the SiC yields during carbothermic reduction from SiO_2 contents in the 1273 K pyrolysis products, powder mass yields from the products after carbothermic reduction, and SiC contents in the resulting powders. The SiC molar yield from SiO_2 in the SiO_2-C hybrid was 80.3% for sample 1 or 81.9% for sample 2. About 20% of SiO_2 is lost in the form of SiO at the 2073 K reaction. Although the C/SiO_2 molar ratios are beyond 4, these estimated yields are considerably lower than the values (95–100%) expected for a completely homogeneous precursor.[6,9,27]

Thus, the following two-step reaction is appropriate to explain SiC-C sphere formation in this case.[27,28]

$$SiO_2 (g) + C (g) \rightarrow SiO (g) + CO (g) \qquad (1)$$

$$SiO (g) + 2C (g) \rightarrow SiC (g) + CO (g) \qquad (2)$$
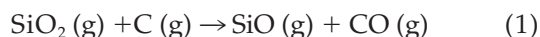
It is plausible that the reaction (1) mainly proceeds in the SiO_2-rich matrix area and the dispersed C domain traps SiO by the reaction (2). In our system, the matrix in the precursor plays the role of Si supplement for the template domains. One major problem is, however, a considerably high carbon content in the matrix estimated. If we assume a C/SiO_2 ratio of 2 in the matrix area and 100% efficiency on localized reactions, 50% of the silicon carbide can be formed at the matrix area at least ($SiO_2 + 2C \rightarrow 0.5SiO + 0.5SiC + 1.5CO$). This is an issue of mass transfer of silicon-containing species (Si, SiO, or SiO_2), corresponding to the disappearance of the matrix area. Further investigation for transient states of the carbothermic reduction process is needed. In particular, such a carbothermic reduction process is highly influenced by the SiO and CO gas pressures surrounding the systems. The effect of chemical environments during the pyrolysis process on SiC yield and morphology requires future investigation as well as the effect of precursor microstructures.

The almost identical SiC yields calculated for samples 1 and 2 suggest the same mechanism for the SiC formation. The morphological difference between the sample 1 powder and the sample 2 powder is possibly due to the difference in the embedded spherical carbon-rich domain nature before the carbothermic reduction process. The carbon domains formed in sample 2 may be dense compared with those formed in sample 1 and prevent SiO diffusion in the core area of domains. The partially aggregated structure observed in sample 2, however, may suggest that the SiC formation process in sample 2 favors the interface reaction between carbon domains and the matrix area.

SUMMARY

By adjusting the kind of the phenolic resin and the gel preparation conditions, resin–silicate gel sheets with unique heterogeneous microstructure are obtained. Asymmetric phase separation between the phenolic resin and silica gels possibly determines such microstructures, which can be maintained during the pyrolysis process up to 1273 K. The obtained SiC particle morphology and the estimated SiC yield suggest a two-step reaction for SiC formation at 2073 K. Despite some unsolved problem in the mass transfer mechanism at 2073 K, the formed SiC particle morphology is certainly controllable by using the starting precursor morphology as an active template.

References

1. Wei, G. C.; Kennedy, C. R.; Harris, L. A. Am Ceram Soc Bull 1984, 63, 1054.
2. Seog, I.-S.; Kim, C. H. J Mater Sci 1993, 28, 3277.
3. Martin, H.–P.; Ecke, R.; Muller, E. J Eur Ceram Soc 1998, 18, 1737.
4. Hasegawa, I.; Nakamura, T.; Motojima, S.; Kajiwara, M. J Sol-Gel Sci Technol 1997, 8, 577.
5. Ueno, S.; Kameda, K.; Yu, J.; Hiragushi, K.; Miura, Y. J Ceram Soc Japan 1998, 106, 688.
6. Tanaka, H.; Kurachi, Y. Ceram Int 1988, 14, 109.
7. Ono, K.; Kurachi, Y. J Mater Sci 1991, 24, 388.
8. Narisawa, M.; Okabe, Y.; Iguchi, M.; Okamura, K.; Kurachi, Y. J Sol-Gel Sci Technol 1998, 12, 143.
9. Narisawa, M.; Okabe, Y.; Okamura, K.; Kurachi, Y. J Ceram Soc Japan 1999, 107, 285.
10. Haraguchi, K;. Usami, Y;. Ono, Y. J Mater Sci 1998, 33, 3337.
11. Cigna, G. J Appl Polym Sci 1970, 14, 1781.
12. Matsen, M.; Bates, F. Macromolecules 1996, 29, 1091.
13. Morikawa, A.; Yamaguchi, H.; Kakimoto, M.; Imai, Y. Chem Mater 1994, 6, 913.
14. Jackson, C. L.; Bauer, B. J.; Nakatani, A. I.; Barnes, J. D. Chem Mater 1996, 8, 727.
15. Interrante, L. V. Pure Appl Chem 2002, 74, 2247.
16. Vix-Guterl, C.; McEnaney, B.; Ehrburger, P. J Eur Ceram Soc 1999, 19, 427.

17. Sung, I.-K.; Yoon, S.-B.; Yu, J.-S.; Kim, D.-P. Chem Commun 2002, 14, 1480.
18. Cheng, D.-P.; Wu, Z. Z.; Ning, L.; Interrante, L. V.; Larkin, D. J. Abstract of Papers of the American Chemical Society, 224: 031-MTLS Part 1, Aug. 18, 2002.
19. Fitzer, E.; Schafer, W. Carbon 1970, 8, 353.
20. Tanaka, K.; Ohzeki, K.; Yamabe, T.; Yata, S. Synth Met 1984, 9, 41.
21. Trick, K. A.; Saliba, T. E. Carbon 1995, 33, 1509.
22. Nakanishi, K.; Soga, N. J Non Cryst Solids 1992, 139, 1.

23. Jiang, P.; Hwang, K. S.; Mittleman, D. M.; Bertone, J. F.; Colvin, V. L. J Am Chem Soc 1999, 121, 11630.
24. Nakanishi, K. J Sol-Gel Sci. Tech 2000, 19, 65.
25. Tanaka, H.; Iyi, N. J Am Ceram Soc 1995, 78, 1233.
26. Kim, Y.-W.; Mitomo, M.; Hirotsuru, H. J Am Ceram Soc 1997, 80, 99.
27. Kevorkijan, V. W.; Komac, M.; Kolar, D. J Mater Sci 1992, 27, 2705.
28. Seo, W.-S.; Koumoto, K. J Am Ceram Soc 1996, 79, 1777.